PHYSICAL REVIEW E **74**, 025401(R) (2006)

Radiative opacity of gold plasmas studied by a detailed level-accounting method

Jiaolong Zeng and Jianmin Yuan
Department of Physics, National University of Defense Technology, Changsha 410073, People's Republic of China
(Received 30 March 2006; published 3 August 2006)

There are systematic discrepancies unexplained so far between theory and experiment for opacities of mid- and high-Z plasmas. To address this issue, we investigated the radiative opacity of gold plasmas by using a detailed level-accounting (DLA) method, in which various physical effects can be taken into account. In this work, we studied in detail the effects of core-valence electron correlation and linewidth on the opacity of gold plasmas. Our DLA results correctly explain the relative intensity of the two strong absorption peaks located near the photon energies of 70 and 80 eV, which was experimentally observed by Eidmann *et al.* [Europhys. Lett. **44**, 459 (1998)]. Meanwhile, the DLA results showed that effects of saturation for the strong individual lines are evident in the transmission spectrum.

DOI: 10.1103/PhysRevE.74.025401 PACS number(s): 52.25.Os

Radiative opacity is of great utility in the study of inertial confinement fusion (ICF) [1], stellar physics [2], and x-ray lasers. Due to its importance, much effort has been made in this research field. For the opacity of light elements such as Al, good agreement is obtained between theory and experiment [3–6]. For mid- and high-Z elements, however, there are systematic discrepancies unexplained so far [7–9]. Are these discrepancies caused by theoretical approximations or experimental uncertainties? In order to solve this problem, combined efforts from both sides should be made. Experimentally, Iglesias [10] pointed out that unresolved structures in the backlight spectrum can introduce significant errors in the inferred transmission. Theoretically, some physical effects that have been treated approximately or missed in theoretical models may affect the accuracy of the opacity determination. For example, some discrepancies are supposed to be a consequence of line saturation effect [10], which can better be reproduced by detailed level-accounting (DLA) models rather than statistical ones.

Gold (Au) is an element of particular interest for indirectly driven ICF, where laser radiation heats the inside of a Au *Hohlraum* producing a plasma that emits intense x rays. In designing the *Hohlraum* and target, radiative opacity is a crucial physical parameter. Recently, Jones *et al.* [11] measured the absolute albedos of *Hohlraums* from Au or from high-Z Au mixtures. Their results showed that the albedo of Au predicted by using the opacity of supertransition arrays (STAs) agrees better with their experimental values than that obtained by using an average atom (AA) model. Dewald *et al.* [12] carried out the first Au *Hohlraum* experiments on the National Ignition Facility (NIF) using the initial four laser beams to test radiation temperature limits imposed by plasma filling. Some research has been carried out on the opacity of Au plasmas, both experimentally and theoretically. Eidmann *et al.* [8] measured the opacity of a Au plasma at density of $\sim 0.01\ \mathrm{g/cm^3}$ and temperature of ~ 20 eV. By mixing appropriate elements with Au, Orzechowski *et al.* [13] experimentally demonstrated the increase of the Rosseland mean opacity of the mixtures. Theoretical research reported in the literature has used statistical models such as unresolved transition array (UTA) [14], STA [8], and AA [15] models. For detailed descriptions of these models, see Refs. [16,17] for UTA and Ref. [18] for STA. To the best of our knowledge, no work has been reported by using a detailed term-accounting (DTA) or DLA model, although such a method is very important to correctly understand and accurately design relevant experiments.

In this work, we investigated the opacity of a Au plasma under the experimental condition of Eidmann *et al.* [8] by using a DLA model. This method can give not only the Rosseland and Planck opacities, but also all detailed absorption structures of the spectrally resolved opacity. In the study of radiative transfer, one usually needs the group opacity. Detailed spectrally resolved opacity helps one to build a multigroup model [19].

The outline of the theoretical method is as follows. For a plasma of temperature T and mass density ρ in local thermodynamic equilibrium (LTE), the fraction of radiation transmitted at photon energy $h\nu$ with respect to some incident source of arbitrary intensity is given by

$$F(h\nu) = e^{-\rho\kappa'(h\nu)L}, \tag{1}$$

where L is the path length traversed by the light source through the plasma and $\kappa'(h\nu)$ is the radiative opacity (the prime on the opacity denotes that stimulated emission has been included), which is given by

$$\rho\kappa'(h\nu) = \sum_i \left(\sum_{ll'} N_{il}\sigma_{ill'}(h\nu) + \sum_l N_{il}\sigma_{il}(h\nu) + \kappa_{ff}(h\nu) + \kappa_{scatt}(h\nu) \right)(1 - e^{-h\nu/kT}), \tag{2}$$

where $\sigma_{ill'}(h\nu)$ is the photoexcitation cross section from level l to l' of ion i, $\sigma_{il}(h\nu)$ is the photoionization cross section from level l of ion i, $\kappa_{ff}(h\nu)$ and $\kappa_{scatt}(h\nu)$ are the free-free and scattering opacities, and N_{il} is the population for level l of ion i obtained from the Boltzmann distribution function, while the fraction of different ionization stages is obtained by solving the ionization equilibrium equation in LTE. The ionization potential depression is considered by using the Debye-Huckel model [4]. The photoexcitation cross section for a bound-bound transition from level l to l' can be expressed in terms of the oscillator strength $f_{ill'}$ of the spectral line as

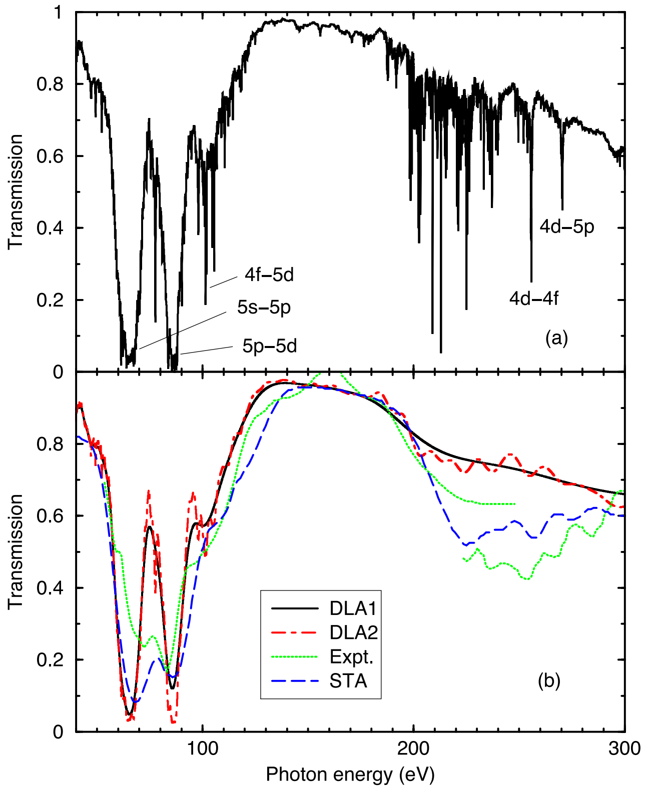

FIG. 1. (Color online) Transmission of a Au plasma at a temperature of 22.5 eV and a density of 0.007 g/cm^3: (a) DLA results and (b) with instrumental broadening included. The experimental and STA data are taken from Ref. [8].

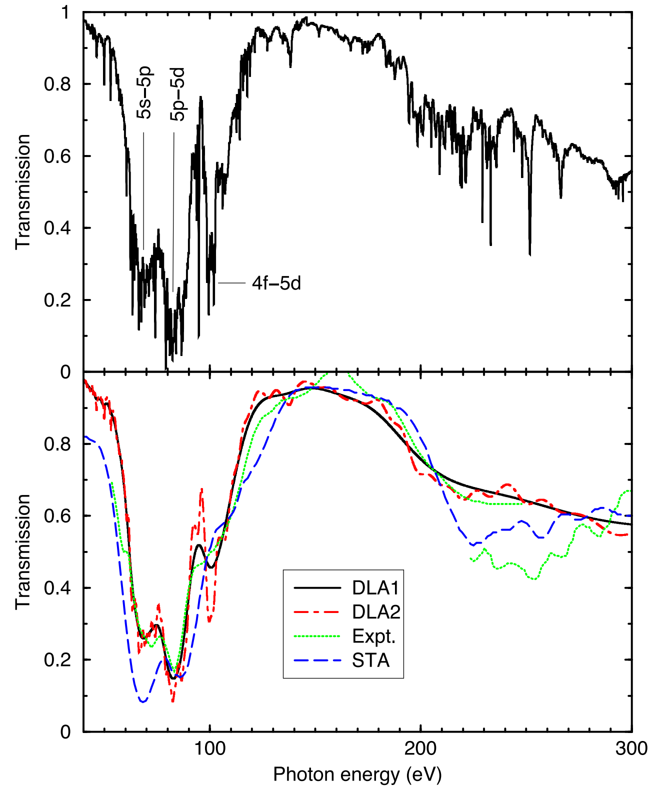

FIG. 2. (Color online) The same as in Fig. 1, while extensive core-valence electron correlations have been included in the calculation of bound-bound transitions: (a) DLA results and (b) with instrumental broadening included. In this figure, the physical effects such as core-valence correlations and autoionization widths have been considered, while in Fig. 1, these effects have not been included.

$$\sigma_{ill'}(h\nu) = \frac{\pi h e^2}{m_e c} f_{ill'} S(h\nu), \quad (3)$$

where h is Planck's constant, c is the speed of light in vacuum, e is the electron charge, and m_e is the electron rest mass. S is the line shape function, which is taken to be a Voigt profile [20].

To obtain accurate opacity, one needs accurate atomic data including the energy levels, oscillator strengths, photoionization cross sections, etc. These basic parameters are also important research fields of current work [21,22]. The atomic data required in the present work are obtained using the flexible atomic code (FAC) developed by Gu [23]. A fully relativistic approach based on the Dirac equation is used throughout the package and thus the relativistic effect has naturally been included. In the following, we present the effects of core-valence electron correlation and line saturation on the accuracy of opacity. For a Au plasma at a temperature of 22.5 eV and a density of 0.007 g/cm^3, the dominant ion types are Au^{8+}–Au^{12+}, accounting for 7.6%, 30.8%, 34.4%, 16.2%, and 9.8%, respectively.

The effect of core-valence electron correlations can easily be seen from the comparison of Figs. 1 and 2 which show the transmission for a Au plasma under the above plasma condition using different sizes of correlations to calculate the oscillator strengths of bound-bound transitions. In the two figures, the treatment of the bound-free, free-free, and scattering processes is the same, while it is different for that of the bound-bound absorption as described below. In Fig. 1, the oscillator strengths of all individual spectral lines have been obtained by considering every necessary transition array one by one for every ion in the plasma. The interactions between all levels generated by all possible couplings within the same configuration have been included. The maximum principle quantum number has been considered up to 12 according to the ionization potential depression. In Fig. 2, however, extensive configuration interactions (CIs) have been included to obtain the oscillator strengths. To illustrate the scale of the CIs, we take Au^{11+} as an example. Its ground configuration is ([Ni]$4s^2 4p^6$)$4d^{10}4f^{14}5s^2 5p^6$. Electron correlations have been included among the following configurations: $5p^6$, $5p^5nl$, $5snl$, $4f^{13}nl$, $4d^9 nl$, $5p^4 nln'l'$, $5s5p^5 nln'l'$, $4f^{13}5p^5 5dnl$, $4d^9 5p^5 5dnl$, $5p^3 5d^2 nl$, $5s5p^4 5d^2 nl$, $4f^{13}5p^4 5d^2 nl$, and $4f^{12}5p^5 5d^3$ $(nl, n'l' = 5d, 5f, 5g, 6s, 6p, 6d)$. Besides the valence electron correlations, most of the interactions are contributed by core-valence electron correlations, because they are due to excitations of $4d$, $4f$, $5s$, and/or $5p$ core subshells. The remaining oscillator strengths required in the calculation of opacity are treated in the same way as in Fig. 1.

Figures 1(a) and 2(a) show our DLA transmission obtained by the two different sizes of correlations described above. The path length L is taken to be 2.5×10^{-5} cm to obtain the results. One can see that the spectrum is highly resolved and shows complex line structures. The line saturation effect is evident for the strong absorption lines. This effect occurs as a result of nonlinear behavior and strongly depends on the ratios of the linewidths to the experimental spectral resolution [5]. To directly compare with the experiment, one should consider the instrumental broadening effect, which can be done by convoluting the DLA transmission over a Gussian function, with full width at half maximum corresponding to the spectrometer resolution. In their experiment, Eidmann *et al.* [8] measured with 1000 and 5000 lines/mm transmission gratings, corresponding to experimental spectral resolution of 1 and 0.2 nm, respectively. In Figs. 1(b) and 2(b), the solid line refers to the result of a resolution of 1 nm (DLA1), the dot-dashed line to that of 0.2 nm (DLA2), the dotted line to the experimental spectrum, and the long-dashed line to the STA result [8]. When comparing with the experiment, DLA1 corresponds to the lower photon energy range (<220 eV), and DLA2 to above 200 eV. We discuss the spectrum in the lower (<130 eV) and higher (>200 eV) photon energy ranges, where there are rich spectral line structures.

To begin with, pay attention to the two strongest absorption peaks near photon energies of 70 and 80 eV. In Fig. 1(b), the DLA treatment results in a narrower absorption feature than the STA in the energy region of 70–80 eV. The relative intensity of the two peaks predicted by both theories is reversed compared to the experiment. The two peaks originate mainly from the absorptions of 5*s*-5*p* and 5*p*-5*d* transitions, respectively. Both types of transition have contributions to the two peaks; however, the peak near 70 eV is mainly due to 5*s*-5*p* and the other one near 80 eV to 5*p*-5*d*. The structures near 100 eV are mainly caused by 4*f*-5*d* transitions. When we include extensive core-valence correlations, our DLA transmission is in good agreement with the experiment, not only for the detailed structures, but also for the relative intensity of the two peaks. The effect of core-valence electron correlations is to lower 5*p*-5*d* absorption, but to enhance that of 4*f*-5*d*. This effect not only changes the positions of the individual lines, but also modifies the distribution of their intensity.

Second, look at the transmission above 200 eV. In this energy range, the peaks around 255 and 300 eV are mainly due to 4*d*-4*f* and 4*d*-5*p* absorptions, respectively, although 4*f*-6*g* and 4*f*-7*g* transitions have contributions as well. Around 200 eV, the structures are mainly caused by 4*f*-5*g* transitions. Besides line absorption, the contribution of direct photoionization begins to increase with the opening of the 4*f* ionization channel. In this energy region, differences between the DLA results shown in Figs. 1 and 2 are caused by a combined effect of core-valence electron correlation and linewidth. We have just demonstrated the former effect in detail in the last paragraph; thus we focus our attention on the latter below. In Fig. 1, we have included the linewidths caused by electron impact and Doppler broadening mechanisms. For the lines below 120 eV, this consideration is appropriate, whereas it is not true for lines above 200 eV, whose upper levels are autoionized states. We have carried out calculations on the autoionization width of some autoionized levels by using the Dirac atomic *R*-matrix code (DARC) [24] and FAC [23]. A fair agreement is found between the two theories, while the FAC predicts generally larger widths than the DARC. The results show that a typical value is about 0.4 eV except for the 4*d*-4*f* giant resonances, whose width can be more than 1 eV. To simplify the calculation, we take it to be 0.4 eV. The linewidth caused by electron impact broadening is less than 0.05 eV, while the Doppler width is even smaller. The autoionization width is, therefore, the largest among all broadening mechanisms for these inner-shell transition lines. With the effects of core-valence correlation and linewidth considered, our DLA results agree better with the experiment.

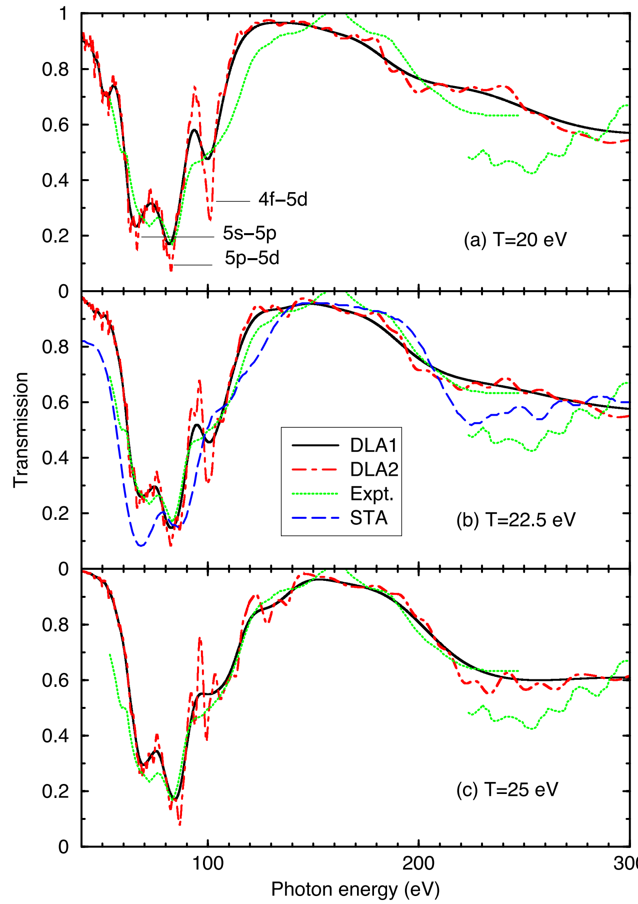

FIG. 3. (Color online) Transmission of Au plasmas at a density of 0.007 g/cm^3 and temperatures of (a) 20, (b) 22.5, and (c) 25 eV, respectively.

To have a better understanding of the plasma condition in the experiment, we have also calculated the transmission at temperatures of 20 and 25 eV, which is shown in Fig. 3. One can see that the spectrum is very sensitive to the temperature, both for the overall structures and for the relative intensity of the two strongest peaks. Comparing the theoretical transmission with the experiment, one can conclude that the experimental spectrum has mixed characteristics of the three temperatures. In the photon energy range of 60–110 eV, the spectrum of 22.5 eV agrees best with the experiment, while below 60 eV, the experimental spectrum has an ingredient of 20 eV or even lower temperature. Above the photon energy of 200 eV, the temperature of the experimental sample seems to be closer to 25 eV. In the whole photon energy range, the transmission of 22.5 eV accords best with the experiment. It is evident that nonhomogeneity of the experimental sample and temperature gradient existed in the experiment [8]. This might be the main reason for the differences between our DLA results and the experiment in the photon energy ranges of 40–60 and 110–130 eV.

The strong sensitivity to the temperature implies that the transmission spectrum is an ideal diagnostic tool for the temperature of plasmas. Past experiments have used low-Z materials such as aluminum as a temperature diagnostic (for example, see [25]). Accurate opacity of low-Z materials can be obtained by using a DTA or DLA method. One can deduce the temperature of plasmas by comparing the theoretical spectrum with the experiment. However, such a tracer element for temperature diagnostics does not always fit for high-Z materials. Because of their complex structures, high-Z elements usually have absorptions over a wide energy range. As a result, they will contaminate the spectrum of the tracer element and then affect the accuracy of diagnosis. In this case, the transmission spectrum obtained by a DLA model can be used as a tool for temperature diagnostics.

In summary, the radiative opacity of Au plasmas has been investigated by using a DLA method. Fine treatment for every true individual line by considering physical effects such as relativity, core-valence electron correlation, and autoionization width is essential to reproduce the fine structures of the transmission spectrum of heavy elements, although there are so many individual lines that statistical models can often give reasonable simulations for the general characteristics. Our DLA prediction correctly explains the relative intensity of the two strong peaks due to $5s$-$5p$ and $5p$-$5d$ absorption. Above 200 eV, the effect of the autoionization width plays a role in the transmission spectrum. The transmission predicted by an accurate DLA method can also serve as a temperature diagnostic tool for high-Z plasmas.

This work was supported by the Program for New Century Excellent Talents in University (NCET) and the National Natural Science Foundation of China under Grants No. 10474138 and No. 10204024.

[1] E. Storm, J. Fusion Energy **7**, 131 (1988); R. L. Kauffman *et al.*, Phys. Rev. Lett. **73**, 2320 (1994).
[2] F. J. Rogers and C. A. Iglesias, Science **263**, 50 (1994); C. A. Iglesias *et al.*, Astrophys. J. **445**, 855 (1995).
[3] T. S. Perry *et al.*, Phys. Rev. Lett. **67**, 3784 (1991).
[4] Jiaolong Zeng, Fengtao Jin, Jianmin Yuan, and Qisheng Lu, Phys. Rev. E **62**, 7251 (2000).
[5] C. A. Iglesias, J. K. Nash, M. H. Chen, and F. J. Rogers, J. Quant. Spectrosc. Radiat. Transf. **51**, 125 (1994).
[6] J. Abdallah and R. E. H. Clark, J. Appl. Phys. **69**, 23 (1991).
[7] T. S. Perry *et al.*, J. Quant. Spectrosc. Radiat. Transf. **54**, 317 (1995).
[8] K. Eidmann, A. Bar-Shalom, A. Saemann, and G. Winhart, Europhys. Lett. **44**, 459 (1998).
[9] C. A. Iglesias, M. H. Chen, V. Sonnad, and B. G. Wilson, J. Quant. Spectrosc. Radiat. Transf. **81**, 227 (2003).
[10] C. A. Iglesias, J. Quant. Spectrosc. Radiat. Transf. **99**, 295 (2006).
[11] O. S. Jones *et al.*, Phys. Rev. Lett. **93**, 065002 (2004).
[12] E. L. Dewald *et al.*, Phys. Rev. Lett. **95**, 215004 (2005).
[13] T. J. Orzechowski, M. D. Rosen, H. N. Kornblum, J. L. Porter, L. J. Suter, A. R. Thiessen, and R. J. Wallace, Phys. Rev. Lett. **77**, 3545 (1996).
[14] J. Yan and Z. Q. Wu, Phys. Rev. E **65**, 066401 (2002).
[15] Y. S. Sun, X. J. Meng and S. T. Zheng, Nucl. Sci. Tech. **8**, 6 (1997).
[16] C. Bauche-Arnoult, J. Bauche, and M. Klapisch, J. Opt. Soc. Am. **68**, 1136 (1978).
[17] C. Bauche-Arnoult, J. Bauche, and M. Klapisch, Adv. At. Mol. Phys. **23**, 131 (1987).
[18] A. Bar-Shalom, J. Oreg, W. H. Goldstein, D. Shvarts, and A. Zigler, Phys. Rev. A **40**, 3183 (1989).
[19] Rodolphe Turpault, J. Quant. Spectrosc. Radiat. Transf. **94**, 357 (2005).
[20] Jiaolong Zeng, Jianmin Yuan, and Qisheng Lu, Phys. Rev. E **64**, 066412 (2001).
[21] C. Brandau *et al.*, Phys. Rev. Lett. **91**, 073202 (2003).
[22] D. Dauvergne *et al.*, Phys. Rev. Lett. **90**, 153002 (2003).
[23] M. F. Gu, Astrophys. J. **582**, 1241 (2003).
[24] P. H. Norrington and I. P. Grant, J. Phys. B **20**, 4869 (1987).
[25] T. S. Perry *et al.*, Phys. Rev. E **54**, 5617 (1996).